Histones: A Novel Class of Lipopolysaccharide-Binding Molecules†

Luis A. Augusto,‡ Paulette Decottignies,§ Monique Synguelakis,‡ Magali Nicaise,|| Pierre Le Maréchal,§ and Richard Chaby*,‡

UMR-8619 of the National Center for Scientific Research, University of Paris−Sud, 91405 Orsay, France

Received September 11, 2002; Revised Manuscript Received January 11, 2003

ABSTRACT: Unlike soluble and membrane forms of lipopolysaccharide (LPS)-binding proteins, intracellular LPS-binding molecules are poorly documented. We looked for such molecules in a murine lung epithelial cell line. Two proteins with LPS-binding activity were isolated and unambiguously identified as histones H2A.1 and H4 by mass spectrometry. Synthetic peptides representing partial structures indicated that the LPS binding site is located in the C-terminal moiety of the histones. Extending the study, we found that histones H1, H2A, H2B, H3, and H4 from calf thymus are all able to bind LPS. Bindings were specific, and affinities, determined by isothermal titration calorimetry, were (except for H4) higher than that of the LPS-binding antibiotic polymyxin B. In the presence of H2A the binding of LPS to the macrophage cell line RAW 264.7, and the LPS-induced production of TNF-α and nitric oxide by these cells, were markedly reduced. Histones may thus represent a new class of intracellular and extracellular LPS sensors.

During systemic infection, Gram-negative bacteria release in the circulation minute quantities of lipopolysaccharides (LPS),[1] the major structural component of their outer membrane. This leads to a variety of pathophysiological and often fatal disorders termed as the endotoxic shock, for which no satisfying therapy exists (*1*). The pleiotropic effects of LPS culminate in multiple organ dysfunctions, including lung failure, leading to acute respiratory distress syndrome (ARDS) with high mortality rate (*2*). But lungs are not only a target organ of LPS-induced disorders. They represent also another common route of entry of pathogens, and thus of LPS, into the body. Therefore, the host has developed a defense system that includes factors that detect LPS both in the circulation and in the lung alveoli, to inhibit its deleterious effects or to amplify an alarm response. A number of naturally occurring peptides and proteins (magainins, cecropins, bombins, mellitins, etc.) have LPS-binding capacity (*3*−*5*), and these interactions have different effects on endotoxicity, varying from reduction to enhancement. For example, LPS-binding protein (LBP) and hemoglobin (Hb) are known to enhance the biological activities of LPS (*6*, *7*), whereas these activities are considerably reduced by bactericidal permeability-increasing protein (BPI), lysozyme, and lactoferrin (*8*−*10*).

In the lungs, the alveolar fluid contains regulatory molecules that are capable of sensing the environment and amplifying or dampening inflammatory responses. Lung surfactant, which covers the epithelial lining of the alveoli, contains several components that are active participants in the innate defense system. Two hydrophilic components of alveolar surfactant, SP-A and SP-D, are lung collectins that can bind to LPS and to other bacterial components (lipoteichoic acid, mannans), and a role in pattern recognition has been proposed for these collectins (*11*). We demonstrated recently (*12*) that another component of lung surfactant, SP-C, interacts specifically with bacterial LPS. Unlike SP-A and SP-D, SP-C is amphiphilic and is produced exclusively by type II alveolar epithelial cells. The aim of the present investigation was to examine whether this cell type can also produce other LPS-binding proteins of amphiphilic nature. We used the mouse lung epithelial MLE-12 cell line as a model of mouse type II pneumocytes. These studies revealed that two major amphiphilic proteins of these cells with marked LPS-binding activity are the two histones H2A.1 and H4. This may suggest a yet unsuspected role of histones in LPS recognition and thus in LPS-induced effects.

EXPERIMENTAL PROCEDURES

Reagents. The LPSs from *Salmonella minnesota* (rough mutant Re595), egg yolk L-α-phosphatidylcholine (type XV-E), bovine albumin, and DNA partial structures (2-deoxyribose-5-phosphate and mono-, di-, and polynucleotides) were from Sigma Chemical Co. (St. Louis, MO). All HPLC solvents (LiChrosolv grade) were from Merck (Darmstadt, Germany). Tritium-labeled borohydride (481 GBq/mmol) was from Amersham-Pharmacia Biotech (Buckinghamshire, England). The liquid scintillation reagents Aqualyte and Lipofluor were from Baker (Deventer, The Netherlands). Histones H1, H2A, H2B, H3, and H4, extracted from calf thymus, were from Roche Diagnostics (Basel, Switzerland). The custom peptide synthesis service of Neosystem (Strasbourg, France) produced the different synthetic peptides used ($H2A_{8-27}$, $H2A_{28-48}$, $H2A_{49-67}$, $H2A_{71-92}$, $H2A_{96-115}$, $H4_{1-21}$, and $H4_{81-102}$). A single peak was obtained by HPLC analysis

† This work is supported by a grant from the Direction des Systèmes de Forces et de la Prospective (Contract 99.34.033).

* Corresponding author. Tel.: 33-169154830. Fax: 33-169853715. E-mail: richard.chaby@bbmpc.u-psud.fr.

‡ Endotoxin Group.

§ Chimie des Protéines.

|| Modélisation et Ingéniérie des Protéines.

[1] Abbreviations: ITC, isothermal titration calorimetry; LPS, lipopolysaccharide; MALDI-TOF, matrix-assisted laser desorption and ionization-time-of-flight; RP-HPLC, reverse-phase high performance liquid chromatography; SP-C, surfactant protein C.

10.1021/bi0268394 CCC: $25.00
Published on Web 03/13/2003

of the different peptides, and amino acid and mass spectrometric (MALDI) analyses of the peptides were identical to theoretically predicted values.

Preparation of Tritium-Labeled LPS. The labeling was done by a modification (*12*) of a described procedure (*13*): A sample (2 mg) of LPS from *S. minnesota* Re595 was oxidized (150 min, 20 °C) with sodium periodate (3×10^{-2} M). After destruction of the oxidant with 1 M ethylene glycol, aldehyde groups were reduced (18 h at 4 °C) with an ice-cold solution of $NaB[^3H]_4$ (0.46 GBq, 481 GBq/mmol) in 200 μL of ice-cold borate buffer (0.05 M, pH 9.5). Excess sodium borohydride was destroyed with 5 μL of acetic acid. After two washings (centrifugations at 100 000*g* for 15 min) in 400 μL of an ice-cold water−ethanol mixture (1−1 by vol), the radiolabeled [^{3}H]-LPS (9×10^5 cpm/μg; 2×10^3 cpm/pmol) was stored at −20 °C until use. Nitric oxide production induced by 2 and 5 ng/mL of this radiolabeled material in mouse macrophages was not significantly different from that induced by the same concentrations of unlabeled LPS, indicating that the bioactivity of the LPS was not modified by the radiolabeling procedure.

Cellular Experiments. RPMI-1640 and fetal calf serum (FCS) were from Bio Media (Boussens, France). Culture medium (CM) was RPMI-1640 containing 2 mM L-glutamine, 100 IU/mL penicillin, and 100 μg/mL streptomycin. Mouse recombinant interferon gamma (IFN-γ) was from Gibco (Gaithersburg, MD). Analysis of the binding of [^{3}H]-LPS to adherent mouse macrophage (RAW 264.7) and mouse lung epithelial (MLE−12) cell lines was performed as described previously (*14*). The production of nitric oxide was analyzed by the Griess reaction (*15*), and the secretion of TNF-α was determined with an ELISA kit (eBioscience, San Diego, CA).

Extraction of Amphiphilic Components of MLE-12 Cells. The mouse lung adenocarcinoma cell line MLE-12 was cultured in CM supplemented with 5% FCS. Cells recovered after trypsin treatment, washings in 0.15 M NaCl, and centrifugation at 150*g* were extracted twice (1 h at 4 °C) by suspension under mild stirring (5×10^6 cells/mL) in a mixture of chloroform−methanol−1 M HCl (6:4:0.01 by vol) in 5 mL of polypropylene tubes. The upper organic phases recovered after centrifugation (12 000*g*) were pooled. After evaporation to dryness, hydrophilic components and phopholipids were removed by a modification of the method of Beers (*16*). Briefly, the crude material recovered from 2×10^7 cells was sonicated in distilled water (1 mL). A mixture (5 mL) of diisopropyl ether/1-butanol (3:2 by vol) was then added. After stirring (2 h, 4 °C) and centrifugation (1000*g*), the amphiphilic material was isolated in the interphase. The first interphase was re-extracted twice with the organic solvent and once more with water. The material in the interphase was recovered by evaporation of the solvent under a nitrogen stream.

Reverse-Phase HPLC. Fractions of the material extracted from 2×10^7 cells were analyzed by reverse-phase HPLC (RP-HPLC). In a first analysis, the sample was dissolved in 100 μL of solvent A (0.2% trifluoroacetic acid and 75% methanol in water) and applied on a C_{18} column from Waters (μBondapak C_{18}, 10 μm, 300 × 3.9 mm). Analysis was carried out at a flow rate of 0.7 mL/min, first with solvent A for 10 min and then with a linear gradient (2.5% per min for 30 min) of solvent B (0.1% trifluoroacetic acid in 2-propanol) in solvent A. Absorbance was monitored at 225 nm. Further purification of a pool of fractions 2−4 was achieved by RP-HPLC on a 2.1 × 150 mm Vydac (300 Å) C4 column. Proteins were eluted with a linear gradient from 0−70% acetonitrile in 0.1% trifluoroacetic acid over 30 min at a flow rate of 0.3 mL/min. Absorbance was recorded at 215 nm.

MALDI-TOF Mass Spectrometry. One microliter of HPLC-purified protein was mixed with 1 μL of saturated solution of sinapinic acid in 30% acetonitrile and 0.3% trifluoroacetic acid. Samples were loaded into a MALDI-TOF spectrometer (Perseptive Biosystems, Voyager STR-DE) equipped with a nitrogen laser (337 nm). Spectra were obtained in linear mode using delayed extraction. An accelerating voltage of 20 kV was applied. The external standards used for calibration were *E. coli* thioredoxin, cytochrome *c*, and myoglobin.

For analysis of tryptic peptides, 1 μL of HPLC-purified protein was mixed with 1 μL of saturated solution of α-cyanohydroxycinnamic acid in 50% acetonitrile and 0.3% trifluoroacetic acid, and the mixture was loaded on the MALDI plate. Tryptic cleavage was performed either in solution or directly on the plate by adding 2 μL (100 ng) of trypsin (Boehringer, sequence grade quality) in 50 mM ammonium bicarbonate. Spectra were obtained in reflector mode using delayed extraction. The external standards used for calibration were des-Arg bradykinin, [Glu$^+$]-fibrinopeptide B, [Tyr^8]-substance P, ACTH clip 1−17, ACTH clip 18−39, and ACTH clip 1−17.

LPS-Binding Assay. Glass tubes containing phosphatidylcholine (PC) (0.3 mg) alone or mixed with the material to be tested were evaporated to dryness. After sonication with a solution of BSA (60 μL, 1 mg/mL in 0.15 M NaCl), the vesicles were incubated (2 h, 20 °C) under gentle rotation, with [^{3}H]-LPS (3.6×10^5 cpm; 290 μL in 0.15 M NaCl). The density was then adjusted to 1.185 g/mL by addition of 350 μL of a solution of 1.1% NaCl and 46% NaBr. A discontinuous gradient was prepared by sequential addition of 23% NaCl (0.7 mL) and the radioactive suspension (0.7 mL), 20.5% NaCl (0.7 mL), 16.5% NaCl (0.7 mL), and 8% NaCl (0.2 mL). After centrifugation (65 000*g*, 90 min), the radioactivity of collected fractions was determined by liquid scintillation. Vesicles with bound radiolabeled LPS were recovered at the top (1 mL) of the density gradient, whereas unbound [^{3}H]-LPS was found at the bottom. The LPS-binding index of a compound is defined as the radioactivity recovered at the top (1 mL) of the density gradient, expressed as a percentage of the total radioactivity recovered.

A second LPS-binding assay based on the binding of [^{3}H]-LPS to histone-coated or peptide-coated plates was also used: methanolic solution peptides or histones to be tested were evaporated under vacuum in wells of polypropylene microplates. [^{3}H]-LPS (3×10^5 cpm in 100 μL of a solution of 0.6 mg/mL BSA in 0.15 M NaCl) was incubated for 2 h at room temperature in the coated wells. After five washings with 100 μL of saline, the remaining bound radioactivity was measured.

Isothermal Calorimetry. Isothermal titration calorimetry (ITC) measurements were carried out with a VP-ITC calorimeter manufactured by MicroCal Omega Inc. (Northampton, MA) and interfaced with a computer. A homogeneous suspension of LPS Re-595 was prepared by a modification of the method of Shands and Chun (*17*): the

lyophilized LPS (2 mg) was suspended in 1 mL of a 0.05 M Tris-HCl−0.01 M EDTA buffer (pH 7) and sonicated for 1 min. The suspension was then maintained for 1 min at pH 4 by the addition at 4 °C, with stirring, of 22 μL of 0.5 M HCl. The mixture was then neutralized with 11 μL of 1 M NaOH and adjusted to 0.312 mM in a 10 mM phosphate buffer (pH 7.0). The molecular mass of LPS Re-595 was taken to be 2476 Da (*18*). The proteins to be tested were dissolved in a buffer identical to that of LPS. All solutions were thoroughly degassed under vacuum for 5 min with gentle stirring immediately before use. The thermal reference cell was filled with water. A typical ITC experiment consisted of injections of the LPS suspension into the sample cell of the calorimeter (volume 1.4323 mL) containing the protein (15−20 μM). A preliminary 5 μL injection was followed by 27 injections (10 μL and 10 s duration each), with 4 min spacing between injections. All experiments were performed at 25 °C. ITC scans represent the energy required by the calorimeter to maintain a constant temperature during the multi-injection period. Prior to analysis, the heats of dilution, which were determined in a control experiment by injecting the LPS suspension into buffer alone, were subtracted from the heats determined by injection into the protein solutions. Data from the first 5 μL injection, which are unreliable (diffusion from the syringe), were discarded before analysis. The energy exchanged per mole of LPS injected can then be calculated for the different injections and represented as a function of the ratio between LPS and protein. The binding isotherms obtained were fitted to a hypothetical (one or two sites) binding model by Marquardt nonlinear least-squares analysis (Origin 5.0, MicroCal), which yields values of the different binding and thermodynamic parameters such as the intrinsic binding constant (K_b) and the changes in the enthalpy (ΔH) and entropy (ΔS).

Database Search. For peptide mass fingerprinting, monoisotopic masses were used, and a mass tolerance of 50 ppm was allowed. The peptide masses were matched with the theoretical peptide masses of all proteins from mouse of several databases (SwissProt, TrEMBL and GenPep), using different softwares, especially ProFound for the mixture of the two proteins and PeptIdent (Expasy) for the purified proteins.

Data Processing. In some experiments, data were fitted to a four parameter logistic (sigmoid) curve, using the Marquardt−Levenberg curve fitting algorithm provided in the SigmaPlot 2000 program (SPSS Inc., Chicago, IL).

RESULTS

Presence of Amphiphilic LPS-Binding Molecules in a Mouse Lung Epithelial Cell Line. We reported previously that the lung surfactant protein C (SP-C) of mice and other species interacts with bacterial LPSs (*12*). Because SP-C is produced by alveolar epithelial type II cells, it appeared important to determine if this cell type can also produce other LPS-binding proteins. We used the MLE-12 cell line, a lung epithelial cell line deriving from mouse type II pneumocytes, which produces SP-C constitutively (*19*). To recover cellular components with physicochemical features similar to those of the LPS-binding molecule SP-C, we extracted the cells by a procedure identical to that used to recover SP-C from crude mouse surfactant: hydrophobic components extracted from the cells with a chloroform−methanol mixture were submitted to a second extraction in a water/diisopropyl ether/1-butanol mixture (1:3:2 by vol). The amphiphilic material isolated in the interphase of the second extraction was analyzed by reverse-phase HPLC on a C_{18} column, with a linear gradient of 2-propanol running in an aqueous solution of 0.2% trifluoroacetic acid and 75% methanol. Figure 1A shows that six main peaks were detected by this method.

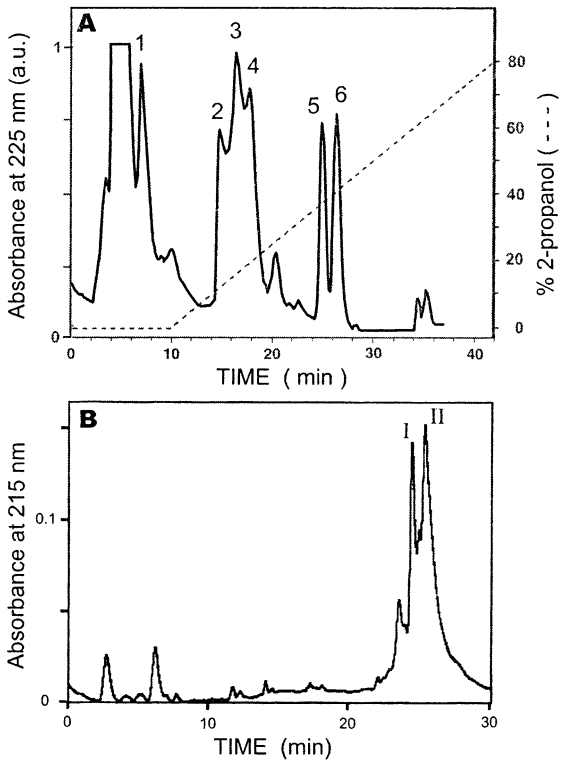

FIGURE 1: RP-HPLC analysis of the material extracted from MLE-12 cells. The material extracted from 2×10^7 MLE-12 cells was dissolved in 100 μL of solvent A (0.2% trifluoroacetic acid and 75% methanol in water) and was separated first (A) by RP-HPLC on a μBondapak C_{18} column (300 × 3.9 mm) with solvent A for 10 min, and then with a linear gradient (2.5% per min, 30 min) of solvent B (0.1% trifluoroacetic acid in 2-propanol) in solvent A, at a flow rate of 0.7 mL/min. A pool of fractions 2−4 was separated further (B) by RP-HPLC on a Vydac C_4 column (2.1 × 150 mm; 300 Å) for 30 min with a linear gradient (0−70% acetonitrile in 0.1% trifluoroacetic acid), at a flow rate of 0.3 mL/min. Absorbance was recorded at 215 nm.

Table 1: LPS-Binding Index of HPLC Fractions of the Amphiphilic Material Extracted from MLE-12 Cells[a]

peak	LPS-binding index (%)
1	1 ± 2
2	2 ± 1
3	52 ± 4
4	24 ± 2
5	2 ± 1
6	14 ± 1

[a] Fractions isolated by HPLC from an extract of 2×10^7 MLE-12 cells (Figure 1) were incorporated into PC/BSA (300 μg/60 μg) vesicles, which were incubated (2 h, 20 °C) with 180 pmol of ^{3}H-LPS (3.6×10^5 cpm). Unbound ^{3}H-LPS was removed by centrifugation of the vesicles on a NaCl/NaBr gradient. The LPS-binding index of the fractions is defined as the percentage of radiolabeled LPS bound to the vesicles. The percentage of radiolabeled LPS bound to empty vesicles of PC/BSA (11 ± 4%) was subtracted from the data. Results are the mean ± SD of duplicates.

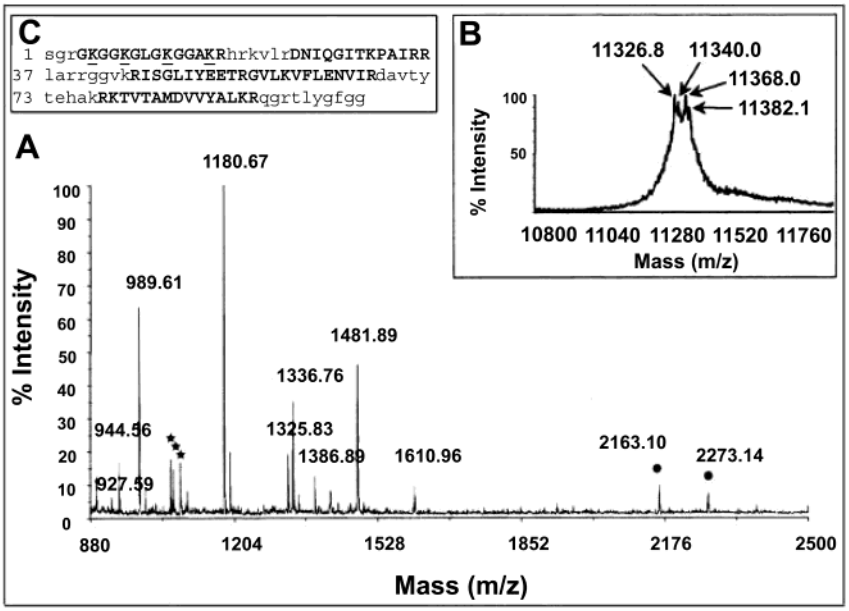

FIGURE 2: Analysis of peak I by MALDI-TOF mass spectrometry. Trypsin-treated (A) and untreated (B) peak I were analyzed by MALDI-TOF mass spectrometry. Peaks marked with a star and with a point correspond to contamination by keratin and to autolysis products of trypsin, respectively. All masses correspond to $[M + H]^+$ ions. (C) Attributed amino acids (bold capitals) in sequences covered by Peptide Mass Fingerprinting of histone H4. Potential acetylation sites are underlined.

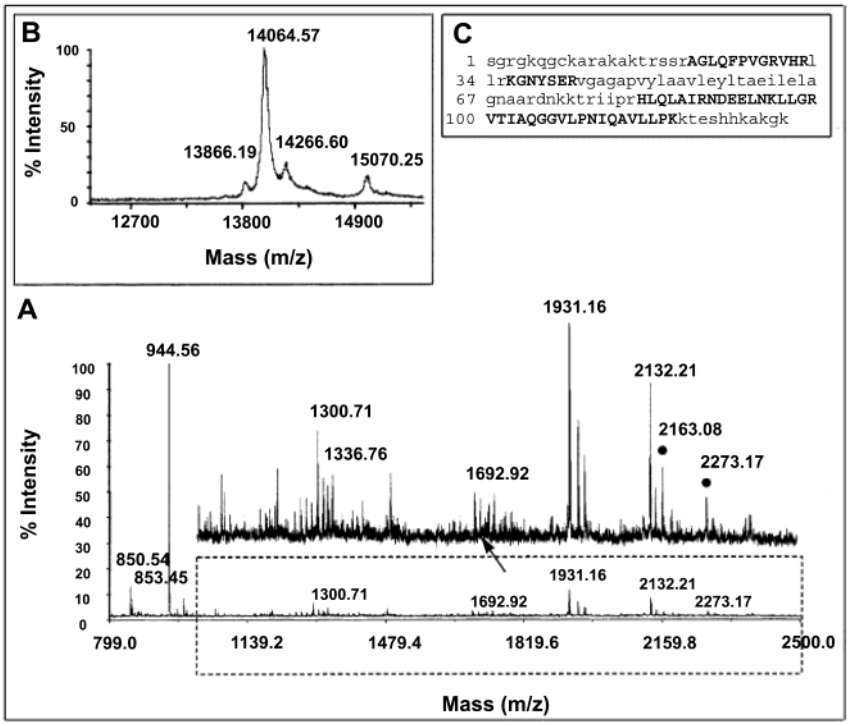

FIGURE 3: Analysis of peak II by MALDI-TOF mass spectrometry. Trypsin-treated (A) and untreated (B) peak II were analyzed by MALDI-TOF mass spectrometry. Peaks marked with a point correspond to autolysis products of trypsin. (C) Attributed amino acids (bold capitals) in sequences covered by Peptide Mass Fingerprinting of histone H2A.1.

The six fractions, isolated from an extract of 2×10^7 cells, were evaporated to dryness and incorporated into lipid vesicles, and the LPS-binding capacity of the corresponding material was analyzed with [^{3}H]-LPS. We used a technique described previously (*12*) in which putative LPS-binding proteins are incorporated in lipid vesicles, and after incubation with radiolabeed LPS, binding is detected after separation of unbound LPS on a density gradient. The results in Table 1 clearly show that the ability to bind LPS is essentially found in the poorly resolved compounds 3 and 4.

Identification of the LPS-Binding Molecules. A pool of the fractions 2−4 was first analyzed by matrix-assisted laser desorption and ionization-time-of-flight (MALDI-TOF) mass spectrometry. Two major proteins were found, with average molecular masses of 14 064 and about 11 350 Da, respectively (data not shown). The fraction was then submitted to a trypsin treatment to identify the proteins by peptide mass fingerprinting and sequence database searching (data not shown). We found that the resulting peptides matched two histones, known as H2 and H4, with calculated masses (about

14 and 11 kDa, respectively) consistent with those actually measured.

To confirm this preliminary result obtained from the mixture of the two proteins, the same work was performed on each protein after purification by RP-HPLC on a C_4 column. Two major peaks (I and II) were isolated (Figure 1B). Both fractions were able to bind ^{3}H-LPS: fractions I and II isolated from 4×10^7 cells exhibited LPS-binding indexes of 52.4 and 57.9%, respectively. The two fractions were analyzed by peptide mass fingerprinting as described above. The results obtained for fraction I are presented in Figure 2A. Eight tryptic peptides matched very well the sequence of the mouse histone H4, with 63.7% of the sequence covered (Figure 2C). Since histones are basic proteins containing a number of tryptic cleavage sites, trypsin treatment generated several small peptides (less than 5−6 amino acids) that could not be detected by MALDI-TOF analysis. Thus, the percent of sequence coverage obtained is high for a small basic protein, and the identification can be considered as reliable. In addition, it is well-known that histone H4 undergoes several posttranslational modifications such as acetylation and methylation of specific lysine residues (*20*). When we used a database that takes into account these modifications (SwissProt), two peptides containing two or three acetyl lysines could be attributed, all of them located in the N-terminus (positions 4−12 and 9−17), as expected. These results suggest that the protein was heterogeneous in terms of posttranslational modifications. This hypothesis was strengthened by the mass spectrum of the full length protein (Figure 2B) that exhibited a strong heterogeneity, corresponding to monomethylation (+14 Da) or acetylation (+42 Da). Four major peaks were observed at 11 326, 11 340, 11 368, and 11 382 Da, respectively. The calculated mass of the $[M + H]^+$ ion of histone H4 is 11 237 Da, this value being increased by 42 Da (11 279 Da) since the amino terminal serine is known to be acetylated. This species could not be observed as a distinct peak in our mass spectrum. On the other hand, the two major peaks at 13 126 and 11 368 Da could be attributed to histone H4 containing one (theorical mass 11 321 Da) or two (theorical mass 11 363) acetylated lysines, respectively. Moreover, these two species can also be monomethylated, giving peaks at 11 339 and 11 381. H4 has been reported to be mono- or dimethylated solely at Lys20 (*20*). Methylation is therefore localized on a small tryptic peptide (Methyl-KVLR, see Figure 2C) that could not be detected by MALDI-TOF analysis.

The same work was performed on the second protein fraction (fraction II) isolated by RP-HPLC (Figure 3). The corresponding protein was identified as H2A by eight matching peptides and sequence coverage of 44% (Figure 3C). The mass spectrum of the full-length protein (Figure 3B) revealed a more homogeneous protein than H4. A closer scrutiny of the tryptic fragments of fraction II discriminated the different reported variants of histone H2A: the peptides at 1300 (NDEELNKLLGR at position 89−99) and 2132 Da (HLQLAIRNDEELNKLLGR at position 82−99) indicated the presence of an arginine (R) at position 99, which is characteristic of the H2A.1 variant of the histone.

Specificity of LPS−Histone Interactions. To assess that the binding of the two histones with LPS was not due to a contaminant of our preparation and cannot be ascribed to nonspecific interactions, we analyzed the binding of ^{3}H-LPS

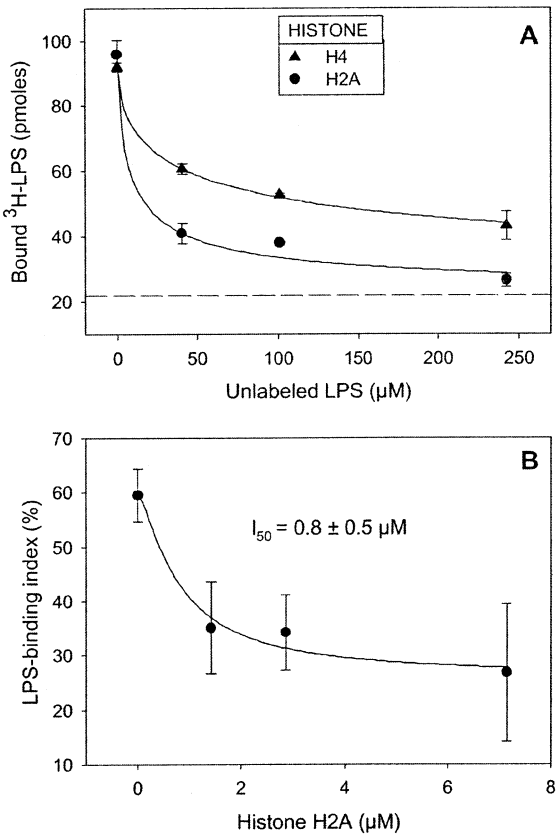

FIGURE 4: Inhibition of the binding of ^{3}H-LPS to histones. Vesicles of PC (300 μg) loaded with H4 (445 pmol) (A) or H2A (179 pmol) (A, B) were incubated (2 h, 20 °C) with ^{3}H-LPS (3.3×10^5 cpm) in the presence of various concentrations of LPS Re-595 in a final volume of 350 μL (A) or with ^{3}H-LPS preincubated (2 h, 20 °C) with various concentrations of histone H2A, in a final volume of 700 μL (B). All incubations were carried out in solutions of BSA (170 μg/mL in 0.15 M NaCl). Unbound ^{3}H-LPS was removed by centrifugation on a NaCl/NaBr density gradient. Results are the mean ± SD of duplicates. The dashed line represents nonspecific binding of ^{3}H-LPS to vesicles. Data were fitted with the four-parameter logistic equation: $Y = Y_m + (Y_0 - Y_m)/(1 + (X/I_{50})^p)$. I_{50} represents the concentration of the competitor at which 50% of the binding is inhibited.

to lipid vesicles loaded with commercially available preparations of histones H2A and H4 isolated from calf thymus, with radiolabeled LPS alone or in competition with unlabeled LPS. The results (Figure 4A) show that ^{3}H-LPS binds efficiently to these preparations of H2A and H4 and that both bindings were dose-dependently inhibited by unlabeled LPS. The binding to H2A was inhibited by lower concentrations of LPS than that to H4 (I_{50} values of 8 ± 3 and 51 ± 6 μM, respectively), indicating a higher affinity of the former for LPS. We also show (Figure 4B) that preincubation of ^{3}H-LPS with H2A blocks dose-dependently the binding of the former to lipid vesicles loaded with H2A. These results indicate a specific interaction between LPS and the two histones.

ITC Analysis of the Interaction of LPS with H2A and H4. Isothermal titration calorimetry was conducted to obtain an accurate evaluation of the affinities of the histones to LPS. In a first experiment, we analyzed histone H2A (from calf thymus). The interaction of H2A with LPS was compared to that of polymyxin B (PMB), a cyclic cationic decapeptide antibiotic from *Bacillus polymyxa*, which interacts efficiently with LPS (*21*) and blocks its biological activities (*22*).

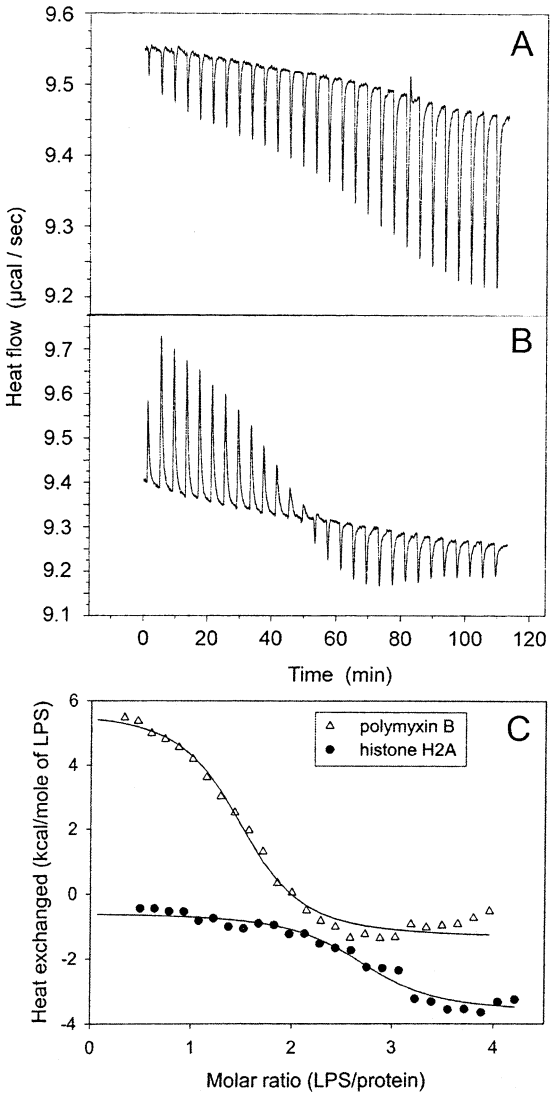

FIGURE 5: ITC analysis of LPS binding to H2A and PMB. Titration scans as a function of time were produced by injection of 10 μL aliquots of 0.312 mM LPS Re-595 into 15.6 μM histone H2A (A) or 16.6 μM of polymyxin B (B) in 10 mM phosphate buffer, at 25 °C. Binding isotherms (C) were derived from the ITC measurements displayed in A and B after subtraction of the heats of dilution. The heat exchanged per mole of LPS injected is plotted vs the LPS/protein ratio. The solid lines represent the best least-squares fit of the values to a theoretical one-site binding model.

Aliquots of LPS were injected into solutions of H2A or PMB contained in the calorimeter cell (V_{cell} = 1.4323 mL). The ITC scans of experiments carried out at 25 °C are given in Figure 5A,B. An exothermic reaction was observed with H2A, whereas with PMB an endothermic binding reaction is followed by a smaller exothermic reaction. In a separate control experiment (not shown), the heat of dilution was obtained by injection of the same aliquots of LPS into buffer alone. Subtraction of the heat of dilution and division by the molar amount of injected LPS yields the molar enthalpy of binding that, when expressed as a function of the LPS/protein molar ratio, represents the binding isotherm at 25 °C (Figure 5C). Fitting the plotted values to a one-site binding model (*23*) allowed the estimation of the free enthalpy change (ΔH_b) and the binding constant (K_b). The dissociation constant K_d was then determined, and change in entropy (ΔS_b) was calculated from the fundamental equation of thermodynamics. We found K_d = 0.78 μM for histone H2A and K_d = 1.07 μM for polymyxin B. Therefore, H2A has a higher affinity for LPS than PMB. Figure 5A,B also shows that binding of H2A to LPS is exothermic whereas that of PMB is endothermic at low concentrations of LPS. It has been reported (*24*) that the endothermic binding of PMB to LPS is driven by hydrophobic interactions. This led us to expect that the exothermic binding of H2A to LPS can be mainly mediated by ionic forces. This hypothesis was actually confirmed by the observation (data not shown) that we were unable to detect by ITC any significant interaction between H2A and LPS at a high ionic concentration (1 M NaCl) at which ionic interactions are known to be neutralized.

Table 2: Inhibition of the Binding of ^{3}H-LPS to Histones H2A and H4 by DNA Partial Structures[a]

compound[b]	concentration (μg/mL)	LPS-binding index (%) H2A vesicles	LPS-binding index (%) H4 vesicles
none		64 ± 3	68 ± 3
2-deoxyribose-5-phosphate	30	66 ± 5	69 ± 3
2′-deoxyguanosine-5′-monophosphate	40	65 ± 2	66 ± 2
dinucleotide	70	65 ± 2	69 ± 2
polynucleotide	0.75	64 ± 2	70 ± 4
	1.5	67 ± 2	44 ± 1
	3	63 ± 2	28 ± 5
	6	35 ± 1	8 ± 1
	12	12 ± 4	6 ± 1

[a] Calf thymus histone H2A (180 pmol) or H4 (445 pmol) were incorporated into PC/BSA (300 μg/60 μg) vesicles, which were preincubated (2 h, 20 °C) with different compounds representing partial DNA structures. The vesicle suspension was then reincubated (2 h, 20 °C) with ^{3}H-LPS (3.6×10^5 cpm). Unbound ^{3}H-LPS was removed by centrifugation of the vesicles on a NaCl/NaBr gradient. The LPS-binding index of the fractions is defined as the percentage of radiolabeled LPS bound to the vesicles. The percentage of radiolabeled LPS bound to empty vesicles of PC/BSA was of 11 ± 4%. Results are the mean ± SD of duplicates. [b] The di-nucleotide is 2′-deoxyadenylyl(3′-5′)-2′-deoxyguanosine-monophosphate. The polynucleotide is a polydeoxyadenylic-thymidylic acid double-stranded alternating copolymer.

The same type of analysis performed with the calf thymus histone H4 indicated a dissociation constant K_d = 5.26 μM. Therefore, the affinity of H4 for LPS is much lower than that of histone H2A. This is consistent with the data of Figure 4A showing that the binding of ^{3}H-LPS to H2A was inhibited by concentrations of unlabeled LPS (I_{50} = 8 μM) lower than those required to inhibit the binding of H4 to LPS (I_{50} = 51 μM).

LPS and DNA Share Common Binding Sites on Histone H2A. Seeing that histones H2A and H4 bind both LPS and DNA, we analyzed the ability of DNA partial structures to inhibit the binding of ^{3}H-LPS to lipid vesicles loaded with H2A. The results in Table 2 show that 2-deoxyribose-5-phosphate, as well as a mono- and a dinucleotide, do not inhibit the binding. In contrast, a marked inhibition is found with a double-stranded polynucleotide. This clearly indicates that LPS and DNA share common binding sites on histone H2A.

Histone Regions Involved in LPS Binding. To localize the LPS-binding sites within the histones, synthetic peptides representing partial structures of murine H2A and H4 were used in a binding assay in which the peptides were adsorbed to the wells of a polypropylene plate. The efficiency of the

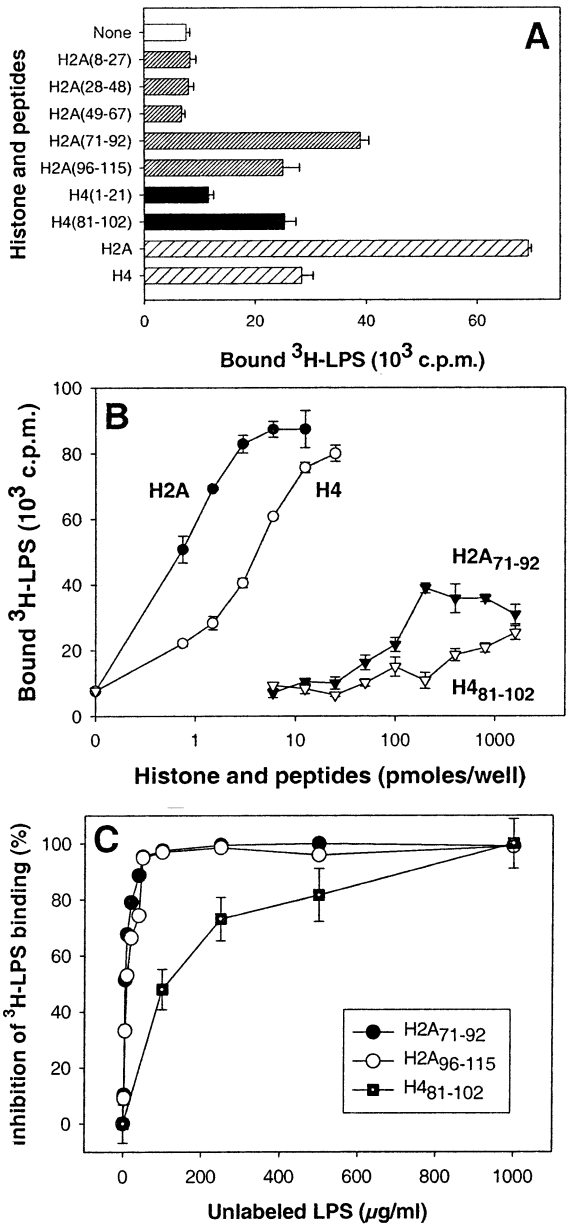

FIGURE 6: Binding of ^{3}H-LPS to histones and peptides derived thereof. Solutions of intact histones or peptides were evaporated in wells of a polypropylene plate. Panel A: 1.5 pmol of histones (coarse hatched bars), 200 pmol of H2A peptides (fine hatched bars), and 1600 pmol of H4 peptides (black bars). Panel B: various amounts of histones and peptides. Incubation of ^{3}H-LPS (3×10^5 cpm in 100 μL of a solution of 0.6 mg/mL BSA in 0.15 M NaCl) was carried out for 2 h at 20 °C in the coated wells. In panel C, 200 pmol of $H2A_{71-92}$ or 400 pmol of $H2A_{96-115}$ or $H4_{81-102}$ were preincubated for 2 h at 20 °C with 100 μL of different concentrations of unlabeled LPS, before addition of ^{3}H-LPS. In all experiments, after incubation with ^{3}H-LPS, the plate was washed with saline, and bound radioactivity, recovered with 100 μL of 10% SDS, was measured. The results are the mean ± SD of triplicates.

adsorption, as estimated by an amino acid assay after strong acid hydrolysis, was high and similar for the different peptides, ranging from a 87% adsorption for $H2A_{71-92}$ to a 99% adsorption for $H2A_{96-115}$. Comparison of the LPS-binding potency of the peptides deriving from H2A (Figure 6A) indicated that ^{3}H-LPS binds essentially to the 71−115 segment of histone H2A, which is located in its C-terminal moiety. The corresponding region of histone H4 ($H4_{81-102}$) also binds ^{3}H-LPS more efficiently than the N-terminal region ($H4_{1-21}$) (Figure 6A). The overall avidities for LPS of the domains deriving from H2A and H4 were clearly different: the results in Figure 6B show that ^{3}H-LPS binds very efficiently to the intact histones H2A and H4 but markedly less to the more avid peptides derived thereof ($H2A_{71-92}$ and $H4_{81-102}$). To ensure that the observed bindings were specific, inhibition experiments with unlabeled ligand were carried out. The results (Figure 6C) indicated that the binding of ^{3}H-LPS was indeed efficiently inhibited by unlabeled LPS. The inhibition curves of the binding to the two H2A-derived peptides were superimposable and were markedly different from that of the H4-derived peptide. This suggests that the 71−92 and 96−115 regions of H2A bind LPS with the same affinity, which appears much higher than that of the 81−102 region of H4.

Table 3: Thermodynamic Parameters for Binding of LPS to Different Proteins[a]

protein	fitting model	K_b (10^5 M^{-1})	ΔH_b (10^3 kcal mol^{-1})	ΔS_b (kcal mol^{-1} deg^{-1})
polymyxin B	one site	9.3	7.1	51
histone H1	two sites	20.8	2.2	36
		1.4	−7.8	3
histone H2A	one site	12.8	3.1	38
histone H2B	one site	41.1	−0.1	30
histone H3	two sites	72.7	2.6	40
		5.4	−4.0	13
histone H4	one site	1.9	3.9	37

[a] A suspension (0.1 mM) of LPS from *S. minnesota* Re-595 was injected (27 injections of 10 μL and 10 s duration each, with 4 min spacing between injections) into the solution of protein (5 μM) at 25 °C. The thermodynamic parameters were calculated by the instrument's software (Origin 5.0, MicroCal) after fitting of the binding data to a hypothetical (one or two sites) binding model.

Interaction of LPS with Other Histones. We used ITC to compare LPS-binding capacities of H2A and H4 to those of the three other known histones: H1, H2B, and H3. Analyses were performed as described above. The results, summarized in Table 3, show that the LPS-binding capacity is not restricted to H2A and H4. The three other histones can also bind LPS, even more efficiently. With two of these (H1 and H3), the best fitting of the data was obtained with a two sites model. The binding constants K_b of the first binding site of histones H1 (2×10^6 M^{-1}), H2B (4×10^6 M^{-1}), and H3 (7×10^6 M^{-1}) are higher than that of H2A (1.3×10^6 M^{-1}). This clearly shows that the capacity to bind LPS is a general feature of histones and that affinities of histones for LPS are generally higher than that of polymyxin B, an antibiotic that efficiently blocks several LPS effects.

Influence of Histone H2A on Cell Binding and Cellular Effects of LPS. To analyze the role of extracellular histones on the cellular effects of LPS, we first examined the influence of histone H2A on the binding of [^{3}H]-LPS to the mouse macrophage cell line RAW 264.7 and to the mouse lung epithelial type II cell line MLE-12. [^{3}H]-LPS was preincubated for 2 h with H2A in the presence or absence of serum, and the mixtures were added to the cells. We found that with RAW 264.7 cells, the binding of [^{3}H]-LPS is higher in the presence of serum and decreases (with or without serum) as a function of the concentration of H2A (Figure 7A). This shows that the LPS receptors of macrophages do not recognize the H2A/LPS complex. In contrast, with MLE-12

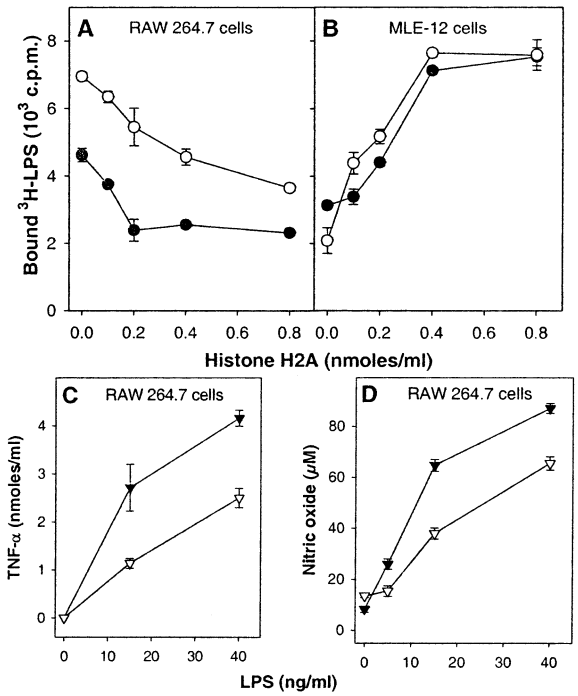

FIGURE 7: Influence of H2A on cellular effects of LPS. In binding experiments (A and B), mixtures (250 μL) of ^{3}H-LPS (3.6×10^5 cpm) preincubated (2 h, 20 °C) with different concentrations of H2A in culture medium, in the presence (○) or absence (●) of 5% FCS, were added to wells coated with RAW 264.7 (A) or MLE-12 (B) cells (10^6 cells/well). After 1 h at 0 °C and three washings with 0.15 M NaCl at 0 °C, the radioactivity of the material recovered with 0.5 mL of 10% SDS was determined. For the estimation of LPS-induced production of TNF-α (C) and nitric oxide (D), various concentrations of *S. minnesota* Re-595 LPS were preincubated (2 h, 20 °C) alone (▽) or with H2A (0.5 nmol/mL) (●). RAW 264.7 cells (5×10^5 cells/well) were cultured (48 h, 37 °C) with these mixtures (500 μL) in culture medium, in the presence of IFN-γ (5 U/mL), and in the absence of serum. Nitric oxide and TNF-α assays were then carried out on culture supernatants. Data are the mean ± SD of triplicates.

cells, the binding of LPS is constitutively low and independent of serum and increases in the presence of H2A, reaching an optimum with about 0.5 nmol/mL (Figure 7B). This suggests the presence of a membrane receptor for H2A on the epithelial MLE-12 cell line, which is able to bind the H2A/LPS complex.

We then examined the influence of histone H2A on the production of inflammatory mediators (TNF-α, NO) induced by LPS in RAW 264.7 cells. Different concentrations of LPS were preincubated for 2 h with 0.5 nmol/mL of H2A, or without H2A, in the absence of serum, and the cells were exposed to these mixtures for 24 h. We found that the presence of H2A markedly reduced the LPS-induced production of TNF-α (Figure 7C) and nitric oxide (Figure 7D). Similar results were obtained in the presence of serum (data not shown). These results clearly indicate an antiinflammatory role of extracellular histones.

DISCUSSION

In this study, we have demonstrated that among amphiphilic proteins of a lung epithelial cell line, the most efficient LPS-binding proteins are the two histones H2A.1 and H4. This finding is reminiscent to an early observation (*25*) showing that the lipid A moiety of LPS binds to a protein of 31 kDa assumed to be a nuclear histone. Several years later, it has been reported (*26*) that the major LPS-binding protein in the brain is an isoform of histone H1 predominantly located at the neuronal cell surface. Our results extend this finding to other histones and to another cell type. The fact that LPS-binding proteins are found in a lung epithelial cell line is of particular physiological relevance insofar as lungs represent one of the major routes of penetration of microorganisms into the body. The release of histones in the lungs can be assumed to take place during apoptosis of lung cells triggered by a variety of agents (*27*), including LPS itself (*28*).

Our analysis of the LPS-binding region of H2A and H4 with synthetic peptides representing partial structures indicated that it is included in the 71−115 region of H2A and covers the 81−102 region of H4. Multi-alignment analysis (Figure 8) of the four nucleosomal histones (H2A, H2B, H3, and H4) indicated that these regions cover a hydrophilic domain of 26 amino acids presenting the highest similarity (region 74−99 of H2A and 77−102 of H4). However, the affinities of isolated partial structures of H2A and H4 were much lower than those of the intact proteins and were hardly measurable by ITC, thus indicating that the three-dimensional parameters of the complete histones are critical for LPS binding. It should be noted that affinities of histones for LPS are remarkably high. Our observation that these affinities are higher than that of polymyxin B, an antibiotic known to block several biological activities of LPS, shows the therapeutic potential of histone analogues that may, as some other LPS-binding molecules, reduce bacterial growth, help bacterial opsonization, or directly block the interaction of LPS with host pro-inflammatory pathways.

The biological relevance of our observations requires that under physiological conditions histones could actually meet LPS. This is in fact the case: it is well-established that histones are not exclusively localized in the cell nucleus. After their biosynthesis in the cytosol by free ribosomes

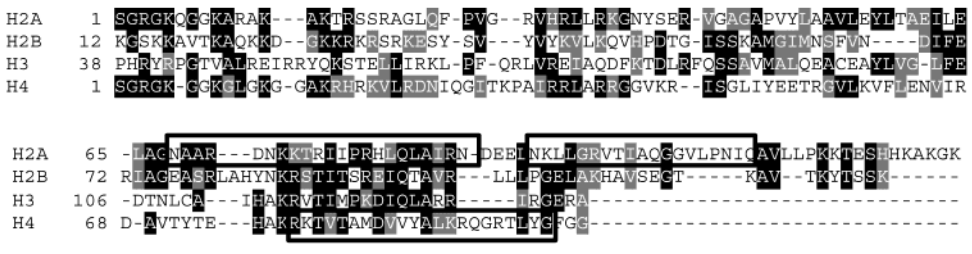

FIGURE 8: Sequence alignment of nucleosomal histones. Sequence alignment of histones H2A, H2B, H3, and H4 generated by the Pattern-Induced Multiple Alignment (PIMA 1.4) program, using maximal linkage alignment data. Representation of amino acid identities (black) and similarities (grey) was generated by the BOXSHADE program. Boxed sequences represent the synthetic peptides $H2A_{71-92}$, $H2A_{96-115}$, and $H4_{81-102}$.

(outside the endoplasmic reticulum), a limited amount of histones is imported into the nucleus via karyopherins (Kaps; also called importins) (*29*), and the excess (unacetylated) histones accumulate in the cytoplasm (*30*−*32*), especially in rapidly regenerating or transcriptionally active cells. The presence of histones on the membrane of various cell types has also been observed (*33*, *34*). Interestingly, it has been reported that LPS increases the amount of membrane associated histones on the cell surface of human monocytes (*35*). Secretion of a portion of the cytoplasmic histones into the extracellular milieu has also been observed (*36*, *37*). Furthermore, extracellular histones can also be found in nucleosomes released from apoptotic cells (*38*, *39*). Therefore, histones are present in the cell nucleus, the cytosol, the plasma membrane, and the extracellular milieu. Our observation that a double-stranded polynucleotide inhibits the binding of LPS to H2A suggests that LPS cannot bind to the nuclear histones of the nucleosome but can bind to histones that are not yet associated to DNA, such as those present in the cytosol or released outside the cell.

The functional role of histones is often viewed mainly in connection with DNA stabilization and gene expression. However, there is growing evidence that histones may be involved in other biological functions, such as stabilization of microtubules (*40*) and bactericidal action (*41*, *42*). For example, buforin, a fragment of histone H2A found in the gastrointestinal tract, is a potent antimicrobial component of the innate host defense system (*43*). Parasin I is another antimicrobial peptide derived from histone H2A (*44*). Concerning histone H4, its 89−102 C-terminal region is identical to the osteogenic growth peptide (OGP), an extracellular mitogen that regulates osteogenesis and hematopoiesis, and its 86−100 region has 80% identity with histogranin, a peptide found in brain and lungs, which protects neurons against over stimulation of the NMDA receptor (*45*) and potentiates the LPS-induced release of IL-1β in alveolar macrophages (*46*). Our observation that peptide $H4_{81-102}$ is an LPS-binding site of H4 suggests that OGP (identical to $H4_{89-102}$) and histogranin (80% identity with $H4_{86-100}$) may also bind LPS.

In view of the high degree of conservation of histones through species evolution (H4 from pea and cow differ in only two amino acids), these molecules may represent a very ancient and ubiquitous element of the innate immune system in the living world by their ability to interact with LPS. Several biological functions can be suggested, depending on the site of this interaction. Extracellular roles of the interaction could be to kill the microorganism to which LPS is attached (bactericidal effect) or to neutralize the pathophysiological effects of cell-free LPS. Our observation that extracellular histone H2A blocks the binding of LPS to macrophages and inhibits the LPS-induced production of TNF-α and NO by these cells (Figure 7) supports this hypothesis. At the cellular level, other possibilities can also be considered, such as LPS-induced signaling after interaction of extracellular LPS with membrane-attached histones or after interaction of internalized LPS with cytosolic receptors. While the response triggered by LPS at the surface of immune cells is well-characterized, that initiated in the cytosol is poorly understood. Nod1 and Nod2 are intracellular proteins that exhibit LPS-binding activity and confer cell responsiveness to LPS via NF-κB activation (*47*). Many other LPS-binding molecules are probably present in the cytosol, and histones may represent a new class of such LPS sensors. There is mounting evidence that after internalization, several agents can translocate to the nucleus and participate directly in regulating gene expression (*48*). In this respect, a rapid localization of LPS in the nucleus has already been reported (*49*, *50*). It is therefore conceivable that after internalization, LPS can be transported into the nucleus by cytosolic histones.

ACKNOWLEDGMENT

We thank Soumaya Hullot-El Moghrabi for cellular extractions and HPLC purifications and Christophe Marchand for mass spectrometry analyses. We are grateful to Michel Desmadril for helpful discussions.

REFERENCES

1. Parrillo, J. E. (1993) Pathogenetic mechanisms of septic shock, *N. Engl. J. Med. 328*, 1471−1477.
2. Fowler, A. A., Hamman, R. F., Good, J. T., Benson, K. N., Baird, M., Eberle, D. J., Petty, T. L., and Hyers, T. M. (1983) Adult respiratory distress syndrome: risk with common predispositions, *Ann. Intern. Med. 98*, 593−597.
3. Wong, P. M., Chugn, S. W., and Sultzer, B. M. (2000) Genes, receptors, signals and responses to lipopolysaccharide endotoxin, *Scand. J. Immunol. 51*, 123−127.
4. Bechinger, B. (1999) The structure, dynamics and orientation of antimicrobial peptides in membranes by multidimensional solid-state NMR spectroscopy, *Biochim. Biophys. Acta 1462*, 157−183.
5. Boman, H. G. (2000) Innate immunity and the normal microflora, *Immunol. Rev. 173*, 5−16.
6. Hailman, E., Lichenstein, H. S., Wurfel, M. M., Miller, D. S., Johnson, D. A., Kelley, M., Busse, L. A., Zukowski, M. M., and Wright, S. D. (1994) Lipopolysaccharide (LPS)-binding protein accelerates the binding of LPS to CD14, *J. Exp. Med. 179*, 269−277.
7. Kaca, W., Roth, R. I., and Levin, J. (1994) Hemoglobin, a newly recognized lipopolysaccharide (LPS)-binding protein that enhances LPS biological activity, *J. Biol. Chem. 269*, 25078−25084.
8. Amura, C. R., Kamei, T., Ito, N., Soares, M. J., and Morrison, D. C. (1998) Differential regulation of lipopolysaccharide (LPS) activation pathways in mouse macrophages by LPS-binding proteins, *J. Immunol. 161*, 2552−2560.
9. Takada, K., Ohno, N., and Yadomae, T. (1994) Binding of lysozyme to lipopolysaccharide suppresses tumor necrosis factor production in vivo, *Infect. Immun. 62*, 1171−1175.
10. Mattsby-Baltzer, I., Roseanu, A., Motas, C., Elverfors, J., Engberg, I., and Hanson, L. A. (1996) Lactoferrin or a fragment thereof inhibits the endotoxin-induced interleukin-6 response in human monocytic cells, *Pediatr. Res. 40*, 257−262.
11. Hoffmann, J. A., Kafatos, F. C., Janeway, C. A., and Ezekowitz, R. A. (1999) Phylogenetic perspectives in innate immunity, *Science 284*, 1313−1318.
12. Augusto, L., Le Blay, K., Auger, G., Blanot, D., and Chaby, R. (2001) Interaction of bacterial lipopolysaccharide with mouse surfactant protein C inserted into lipid vesicles, *Am. J. Physiol. Lung Cell. Mol. Physiol. 281*, L776−L785.
13. Watson, J., and Riblet, R. (1975) Genetic control of responses to bacterial lipopolysaccharides in mice. II. A gene that influences a membrane component involved in the activation of bone marrow-derived lymphocytes by lipipolysaccharides, *J. Immunol. 114*, 1462−1468.
14. Tahri-Jouti, M. A., and Chaby, R. (1990) Specific binding of lipopolysaccharides to mouse macrophages− I. Characteristics of the interaction and inefficiency of the polysaccharide region, *Mol. Immunol. 27*, 751−761.
15. Green, L. C., Wagner, D. A., Glogowski, J., Skipper, P. L., Wishnok, J. S., and Tannenbaum, S. R. (1982) Analysis of nitrate, nitrite, and [15N]nitrate in biological fluids, *Anal. Biochem. 126*, 131−138.
16. Beers, M. F., Bates, S. R., and Fisher, A. B. (1992) Differential extraction for the rapid purification of bovine surfactant protein B, *Am. J. Physiol. 262*, L773−L778.

17. Shands, J. W., Jr., and Chun, P. W. (1980) The dispersion of gram-negative lipopolysaccharide by deoxycholate. Subunit molecular weight, *J. Biol. Chem. 255*, 1221−1226.
18. Caroff, M., Deprun, C., Karibian, D., and Szabo, L. (1991) Analysis of unmodified endotoxin preparations by 252Cf plasma desorption mass spectrometry. Determination of molecular masses of the constituent native lipopolysaccharides, *J. Biol. Chem. 266*, 18543−18549.
19. Horowitz, A. D., Moussavian, B., Han, E. D., Baatz, J. E., and Whitsett, J. A. (1997) Distinct effects of SP-A and SP-B on endocytosis of SP-C by pulmonary epithelial cells, *Am. J. Physiol. 273*, L159−L171.
20. Duerre, J. A., and Buttz, H. R. (1990) in *Protein Methylation* (Paik, W. P., and Kim, S., Eds.) pp 125−138, CRC Press, Boca Raton, FL.
21. Novogrodsky, A., Vanichkin, A., Patya, M., Gazit, A., Osherov, N., and Levitzki, A. (1994) Prevention of lipopolysaccharide-induced lethal toxicity by tyrosine kinase inhibitors, *Science 264*, 1319−1322.
22. Morrison, D. C., and Jacobs, D. M. (1976) Binding of polymyxin B to the lipid A portion of bacterial lipopolysaccharides, *Immunochemistry 13*, 813−818.
23. Wiseman, T., Williston, S., Brandts, J. F., and Lin, L. N. (1989) Rapid measurement of binding constants and heats of binding using a new titration calorimeter, *Anal. Biochem. 179*, 131−137.
24. Srimal, S., Surolia, N., Balasubramanian, S., and Surolia, A. (1996) Titration calorimetric studies to elucidate the specificity of the interactions of polymyxin B with lipopolysaccharides and lipid A, *Biochem. J. 315*, 679−686.
25. Hampton, R. Y., Golenbock, D. T., and Raetz, C. R. (1988) Lipid A binding sites in membranes of macrophage tumor cells, *J. Biol. Chem. 263*, 14802−14807.
26. Bolton, S. J., and Perry, V. H. (1997) Histone H1; a neuronal protein that binds bacterial lipopolysaccharide, *J. Neurocytol. 26*, 823−831.
27. Eneman, J. D., Potts, R. J., Osier, M., Shukla, G. S., Lee, C. H., Chiu, J. F., and Hart, B. A. (2000) Suppressed oxidant-induced apoptosis in cadmium adapted alveolar epithelial cells and its potential involvement in cadmium carcinogenesis, *Toxicology 147*, 215−228.
28. Bingisser, R., Stey, C., Weller, M., Groscurth, P., Russi, E., and Frei, K. (1996) Apoptosis in human alveolar macrophages is induced by endotoxin and is modulated by cytokines, *Am. J. Respir. Cell. Mol. Biol. 15*, 64−70.
29. Muhlhausser, P., Muller, E. C., Otto, A., and Kutay, U. (2001) Multiple pathways contribute to nuclear import of core histones, *EMBO Rep. 2*, 690−696.
30. Chang, L., Loranger, S. S., Mizzen, C., Ernst, S. G., Allis, C. D., and Annunziato, A. T. (1997) Histones in transit: cytosolic histone complexes and diacetylation of H4 during nucleosome assembly in human cells, *Biochemistry 36*, 469−480.
31. Watson, K., Edwards, R. J., Shaunak, S., Parmelee, D. C., Sarraf, C., Gooderham, N. J., and Davies, D. S. (1995) Extra-nuclear location of histones in activated human peripheral blood lymphocytes and cultured T-cells, *Biochem. Pharmacol. 50*, 299−309.
32. Zlatanova, J. S., Srebreva, L. N., Banchev, T. B., Tasheva, B. T., and Tsanev, R. G. (1990) Cytoplasmic pool of histone H1 in mammalian cells, *J. Cell. Sci. 96*, 461−468.
33. Mecheri, S., Dannecker, G., Dennig, D., Poncet, P., and Hoffmann, M. K. (1993) Anti-histone autoantibodies react specifically with the B cell surface, *Mol. Immunol. 30*, 549−557.
34. Khan, I. U., Wallin, R., Gupta, R. S., and Kammer, G. M. (1998) Protein kinase A-catalyzed phosphorylation of heat shock protein 60 chaperone regulates its attachment to histone 2B in the T lymphocyte plasma membrane, *Proc. Natl. Acad. Sci. U S A 95*, 10425−10430.
35. Emlen, W., Holers, V. M., Arend, W. P., and Kotzin, B. (1992) Regulation of nuclear antigen expression on the cell surface of human monocytes, *J. Immunol. 148*, 3042−3048.
36. Watabe, Y., Kuramochi, H., Furuya, Y., Inagaki, N., Seino, S., Kimura, S., and Shimazaki, J. (1996) Identification of histone H2A.X as a growth factor secreted by an androgen-independent subline of mouse mammary carcinoma cells, *J. Biol. Chem. 271*, 25126−25130.
37. Brix, K., Summa, W., Lottspeich, F., and Herzog, V. (1998) Extracellularly occurring histone H1 mediates the binding of thyroglobulin to the cell surface of mouse macrophages, *J. Clin. Invest. 102*, 283−293.
38. Bell, D. A., Morrison, B., and VandenBygaart, P. (1990) Immunogenic DNA-related factors. Nucleosomes spontaneously released from normal murine lymphoid cells stimulate proliferation and immunoglobulin synthesis of normal mouse lymphocytes, *J. Clin. Invest. 85*, 1487−1496.
39. Schwartz, L. M., and Osborne, B. A. (1993) Programmed cell death, apoptosis and killer genes, *Immunol. Today 14*, 582−590.
40. Multigner, L., Gagnon, J., Van Dorsselaer, A., and Job, D. (1992) Stabilization of sea urchin flagellar microtubules by histone H1, *Nature 360*, 33−39.
41. Hirsch, J. G. (1958) Bactericidal action of histone, *J. Exp. Med. 108*, 925−944.
42. Kim, H. S., Cho, J. H., Park, H. W., Yoon, H., Kim, M. S., and Kim, S. C. (2002) Endotoxin-neutralizing antimicrobial proteins of the human placenta, *J. Immunol. 168*, 2356−2364.
43. Park, I. Y., Park, C. B., Kim, M. S., and Kim, S. C. (1998) Parasin I, an antimicrobial peptide derived from histone H2A in the catfish, Parasilurus asotus, *FEBS Lett. 437*, 258−262.
44. Kim, H. S., Yoon, H., Minn, I., Park, C. B., Lee, W. T., Zasloff, M., and Kim, S. C. (2000) Pepsin-mediated processing of the cytoplasmic histone H2A to strong antimicrobial peptide buforin I, *J. Immunol. 165*, 3268−3274.
45. Lemaire, S., Shukla, V. K., Rogers, C., Ibrahim, I. H., Lapierre, C., Parent, P., and Dumont, M. (1993) Isolation and characterization of histogranin, a natural peptide with NMDA receptor antagonist activity, *Eur. J. Pharmacol. 245*, 247−256.
46. Lemaire, I., Yang, H., Cantin, M. F., and Lemaire, S. (1994) Up-regulation of cytokine production in alveolar macrophages by histogranin, a novel endogenous pentadecapeptide, *Immunol. Lett. 41*, 37−42.
47. Inohara, N., Ogura, Y., Chen, F. F., Muto, A., and Nunez, G. (2001) Human Nod1 confers responsiveness to bacterial lipopolysaccharides, *J. Biol. Chem. 276*, 2551−2554.
48. Jans, D. A. (1994) Nuclear signaling pathways for polypeptide ligands and their membrane receptors? *FASEB J. 8*, 841−847.
49. Lucas, R. M., Subramoniam, A., and Aleo, J. J. (1985) Intracellular localization of bacterial lipopolysaccharide using the avidin biotin complex method at the electron microscopic level, *J. Periodontol. 56*, 553−557.
50. Kang, Y. H., Lee, C. H., Monroy, R. L., Dwivedi, R. S., Odeyale, C., and Newball, H. H. (1992) Uptake, distribution and fate of bacterial lipopolysaccharides in monocytes and macrophages: an ultrastructural and functional correlation, *Electron Microsc. Rev. 5*, 381−419.

BI0268394